Academic Open Internet Journal www.acadjournal.com Volume 19, 2006
ISSN 1311-4360

Evaluation of Discrete Cosine Transform based Gradient Vector Flow Active Contours as an efficient tool for boundary mapping of Chromosome spread images

A.Prabhu Britto[1] and Dr. G. Ravindran[2]

[1]Research Scholar, Center for Medical Electronics, Dept. of Electronics and Communication Engineering, Anna University, Chennai 600 025 INDIA

[2]Chairman, Faculty of Information and Communication Engineering
Anna University, Chennai 600 025 INDIA

Abstract: In this research, characterization of Discrete Cosine Transform (DCT) based Gradient Vector Flow (GVF) Active Contours as an efficient boundary mapping technique for chromosome spread images is done. Statistical testing validates the experimental results of characterization. Investigations on a different dataset are carried out to validate the characterized parameters and the parameters are standardized. Further experiments are carried out to evaluate the validity of the standardization using another dataset. Error Quantification justified the successful standardization. It is hence established that DCT based GVF Active Contour is an efficient tool for boundary mapping of chromosome spread images.

Keywords: Gradient Vector Flow, Active Contours, Chromosome, Boundary Mapping, Characterization, Standardization

I. INTRODUCTION

The classical boundary mapping techniques, namely, region growing, relaxation labeling, edge detection and linking suffer from limitations. Usage of only local information may lead to incorrect assumptions during the boundary integration process leading to errors. Noise and artifacts can possibly cause incorrect segmentation or boundary discontinuities in segmented objects [1]. Therefore, this research work used Discrete Cosine Transform (DCT) based Gradient Vector Flow (GVF) Active Contours to obtain accurate segmentation (boundary mapping) results from a class of chromosome spread images having variability in shape, size and other image properties.

Active Contours or Deformable Curves is a high-level boundary mapping technique. Its main advantage is the ability to generate closed parametric curves from images. The incorporation of a smoothness constraint provides robustness to noise and spurious edges. The focus is on parametric deformable curves, which provide a compact, analytical description of object shape. A class of parametric Active Contours called Gradient Vector Flow (GVF) field Active Contours is chosen for boundary mapping in chromosome spread images[2]. Boundary mapping efficiency of GVF Active Contours on chromosome spread images is improved by embedding the DCT into the boundary mapping scheme[3].

II. ACTIVE CONTOUR MODELS

Active Contours also called as Snakes or Deformable Curves, first proposed by Kass[4] are energy minimizing contours that apply information about the boundaries as part of an optimization procedure. They are generally initialized by automatic or manual process around the object of interest. The contour then deforms itself iteratively from its initial position in conformity with nearest dominant edge feature, by minimizing the energy composed of the Internal and External forces, converging to the boundary of the object of interest. The Internal forces computed from within the Active Contour enforce smoothness of the curve and External forces derived from the image, help to drive the curve toward the desired features of interest during the course of the iterative process.

The energy minimization process can be viewed as a dynamic problem where the active contour model is governed by the laws of elasticity and lagrangian dynamics[5], and the model evolves until equilibrium of all forces is reached, which is equivalent to a minimum of the energy function. The energy function is thus minimized, making the model active.

III. FORMULATION OF ACTIVE CONTOUR MODELS

An Active Contour Model can be represented by a curve **c**, as a function of its arc length t,

$$c(t) = \begin{pmatrix} x(t) \\ y(t) \end{pmatrix} \quad \text{-- (1)}$$

with t = [0…1]. To define a closed curve, c(0) is set to equal c(1). A discrete model can be expressed as an ordered set of n vertices as $v_i = (x_i,y_i)^T$ with $v=(v_1,\ldots,v_n)$. The large number of vertices required to achieve any predetermined accuracy could lead to high computational complexity and numerical instability[5].

Mathematically, an active contour model can be defined in discrete form as a curve $x(s) = [x(s), y(s)], s e[0,1]$ that moves through the spatial domain of an image to minimize the energy functional

$$E = \int_0^1 \frac{1}{2}(a\,|x'(s)|^2 + b\,|x''(s)|^2) + E_{ext}(x(s))ds \quad \text{-- (2)}$$

where a and ß are weighting parameters that control the active contour's tension and rigidity respectively[6]. The first order derivative discourages stretching while the second order derivative discourages bending. The weighting parameters of tension and rigidity govern the effect of the derivatives on the snake.

The external energy function E_{ext} is derived from the image so that it takes on smaller values at the features of interest such as boundaries and guides the active contour towards the boundaries. The external energy is defined by

$$E_{ext} = k\,|G_s(x,y) * I(x,y)| \quad \text{-- (3)}$$

where, $G_s(x,y)$ is a two-dimensional Gaussian function with standard deviation s, I(x,y) represents the image, and ? is the external force weight. This external energy is specified for a line drawing (black on white) and positive ? is used. A motivation for applying some Gaussian filtering to the underlying image is to reduce noise. An active contour that minimizes E must satisfy the Euler Equation

$$ax''(s) - bx''''(s) - \nabla E_{ext} = 0 \quad \text{-- (4)}$$

where $F_{\text{int}} = ax''(s) - bx''''(s)$ and $F_{ext} = -\nabla E_{ext}$ comprise the components of a force balance equation such that $F_{\text{int}} + F_{ext} = 0$ -- (5)

The internal force F_{int} discourages stretching and bending while the external potential force F_{ext} drives the active contour towards the desired image boundary. Eq.(4) is solved by making the active contour dynamic by treating x as a function of time t as well as s. Then the partial derivative of x with respect to t is then set equal to the left hand side of Eq.(4) as follows $x_t(s,t) = ax''(s,t) - bx''''(s,t) - \nabla E_{ext}$ -- (6)

A solution to Eq.(6) can be obtained by discretizing the equation and solving the discrete system iteratively[4]. When the solution x(s,t) stabilizes, the term $x_t(s,t)$ vanishes and a solution of Eq.(4) is achieved.

Traditional active contour models suffer from a few drawbacks. Boundary concavities leave the contour split across the boundary. Capture range is also limited. Methods suggested to overcome these difficulties, namely multiresolution methods[7], pressure forces[8], distance potentials[9], control points[10], domain adaptivity[11], directional attractions[12] and solenoidal fields[13], however solved one problem but introduced new ones[14].

Hence, a new class of external fields called Gradient Vector Flow fields[14,15] was suggested to overcome the difficulties in traditional active contour models.

IV. GRADIENT VECTOR FLOW (GVF) ACTIVE CONTOURS

Gradient Vector Flow (GVF) Active Contours use Gradient Vector Flow fields obtained by solving a vector diffusion equation that diffuses the gradient vectors of a gray-level edge map computed from the image. The GVF active contour model cannot be written as the negative gradient of a potential function. Hence it is directly specified from a dynamic force equation, instead of the standard energy minimization network. The external forces arising out of GVF fields are non-conservative forces as they cannot be written as gradients of scalar potential functions. The usage of non-conservative forces as external forces show improved performance of Gradient Vector Flow field Active Contours compared to traditional energy minimizing active contours[14,15].

The GVF field points towards the object boundary when very near to the boundary, but varies smoothly over homogeneous image regions extending to the image border. Hence the GVF field can capture an active contour from long range from either side of the object boundary and can force it into the object boundary. The GVF active contour model thus has a large capture range and is insensitive to the initialization of the contour. Hence the contour initialization is flexible.

The gradient vectors are normal to the boundary surface but by combining Laplacian and Gradient the result is not the normal vectors to the boundary surface. As a result of this, the GVF field yields vectors that point into boundary concavities so that the active contour is driven through the concavities. Information regarding whether the initial contour should expand or contract need not be given to the GVF active contour model. The GVF is very useful when there are boundary gaps, because it preserves the perceptual edge property of active contours [4,15].
The GVF field is defined as the equilibrium solution to the following vector diffusion equation[14],

$$u_t = g(|\nabla f|)\nabla^2 u - h(|\nabla f|)(u - \nabla f) \quad \text{– (7a)}$$

$$u(x,0) = \nabla f(x) \quad \text{– (7b)}$$

where, u_t denotes the partial derivative of u(x,t) with respect to t, ∇^2 is the Laplacian operator (applied to each spatial component of u separately), and f is an edge map that has a higher value at the desired object boundary. The functions in "g" and "h" control the amount of diffusion in GVF. In Eq.(7), $g(|\nabla f|)\nabla^2 u$ produces a smoothly varying vector field, and hence called as the "smoothing term", while $h(|\nabla f|)(u - \nabla f)$ encourages the vector field u to be close to ∇f computed from the image data and hence called as the data term. The weighting functions $g(\cdot)$ and $h(\cdot)$ apply to the smoothing and data terms respectively and they are chosen[15] as $g(|\nabla f|) = m$ and $h(|\nabla f|) = |\nabla f|^2$. $g(\cdot)$ is constant here, and smoothing occurs everywhere, while $h(\cdot)$ grows larger near strong edges and dominates at boundaries. Hence, the Gradient Vector Flow field is defined as the vector field v(x,y)=[u(x,y),v(x,y)] that minimizes the energy functional

$$e = \int\int m({u_x}^2 + {u_y}^2 + {v_x}^2 + {v_y}^2) + |\nabla f|^2 |v - \nabla f|^2 \, dxdy \quad \text{-- (8)}$$

The effect of this variational formulation is that the result is made smooth when there is no data.

When the gradient of the edge map is large, it keeps the external field nearly equal to the gradient, but keeps field to be slowly varying in homogeneous regions where the gradient of the edge map is small, i.e., the gradient of an edge map ∇f has vectors point toward the edges, which are normal to the edges at the edges, and have magnitudes only in the immediate vicinity of the edges, and in homogeneous regions ∇f is nearly zero. μ is a regularization parameter that governs the tradeoff between the first and the second term in the integrand in Eq.(8). The solution of Eq.(8) can be done using the Calculus of Variations and further by treating u and v as functions of time, solving them as generalized diffusion equations [15].

V. DISCRETE COSINE TRANSFORM (DCT) BASED GVF ACTIVE CONTOURS

The transform of an Image yields more insight into the properties of the image. The Discrete Cosine Transform has excellent energy compaction. Hence, the Discrete Cosine Transform promises better description of the image properties. The Discrete Cosine Transform is embedded into the GVF Active Contours. When the image property description is significantly low, this helps the contour model to give significantly better performance by utilizing the energy compaction property of the DCT.

The 2D DCT is defined as

$$C(u,v) = a(u)a(v)\sum_{x=0}^{N-1}\sum_{y=0}^{N-1} f(x,y)\cos[\tfrac{(2x+1)up}{2N}]\cos[\tfrac{(2y+1)vp}{2N}] \text{ -- (11)}$$

The local contrast of the Image at the given pixel location (k,l) is given by

$$P(k,l) = \frac{\sum_{t=1}^{2(2n+1)-1} w_t E_t}{d_{00}} \text{ -- (12) where, } E_t = \frac{\sum_{u+v=t} |d_{u,v}|}{N} \text{ -- (13) and } N = \begin{cases} t+1 & t<2n+1 \\ 2(2n+1)-t & t \geq 2n+1 \end{cases} \text{ -- (14)}$$

Here, w_t denotes the weights used to select the DCT coefficients. The local contrast P(k,l) is then used to generate a DCT contrast enhanced Image[16], which is then subject to selective segmentation by the energy compact gradient vector flow active contour model using Eq.(8).

VI. RESULTS AND DISCUSSION

The chromosome metaphase image (at 72 pixels per inch resolution) provided by Prof.Ken Castleman and Prof.Qiang Wu (Advanced Digital Imaging Research, Texas) was taken and preprocessed. Insignificant and unnecessary regions in the image were removed interactively. Interactive selection of the chromosome of interest was done by selecting a few points around the chromosome that formed the vertices of a polygon. On constructing the perimeter of the polygon, seed points for the initial contour were determined automatically by periodically selecting every third pixel along the perimeter of the polygon.

The GVF deformable curve was then allowed to deform until it converged to the chromosome boundary. The optimum parameters for the deformable curve with respect to the Chromosome images were determined by tabulated studies. The image was made to undergo minimal preprocessing so as to achieve the goal of boundary mapping in chromosome images with very weak edges. The DCT based GVF Active contour is governed by the following parameters, namely, s, µ, a, ß and ?.

s determines the Gaussian filtering that is applied to the image to generate the external field. Larger value of s will cause the boundaries to become blurry and distorted, and can also cause a shift in the boundary location. However, large values of s are necessary to increase the capture range of the active contour. µ is a regularization parameter in Eq.(8), and requires a higher value in the presence of noise in the image. a determines the tension of the active contour and ß determines the rigidity of the contour. The tension keeps the active contour contracted and the rigidity keeps it smooth. a and ß may also take on value zero implying that the influence of the respective tension and rigidity terms in the diffusion equation is low. ? is the external force weight that determines the strength of the external field that is applied. The iterations were set suitably.

GRAPHICAL CHARACTERIZATION RESULTS

DCT based GVF Active Contours were used to boundary chromosome images from chromosome spread images. A few samples are presented here.

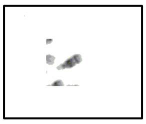
Fig. 1a Sample 1


Fig.2a Sample 2


Fig.3a Sample 3


Fig. 4a Sample 4


Fig. 5a Sample 5


Fig. 6a Sample 6

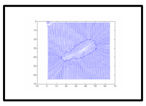
Fig.1b Vector Field

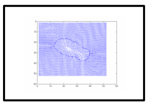
Fig.2b Vector Field

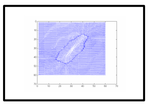
Fig.3b Vector Field

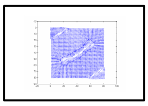
Fig.4b Vector Field

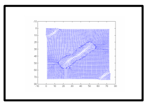
Fig.5b Vector Field

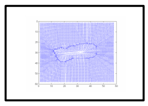
Fig.6b Vector Field


Fig.1c Output Image

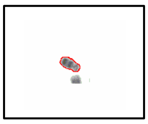
Fig.2c Output Image

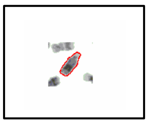
Fig.3c Output Image


Fig.4c Output Image

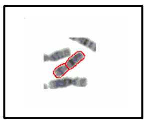
Fig.5c Output Image


Fig.6c Output Image

The figures show original chromosome image samples, their corresponding DCT based GVF fields and boundary mapped chromosome images as output images. For example, Fig.1a shows an original chromosome image sample, Fig.1b shows its corresponding Vector Field and Fig.1c shows its boundary mapped output image, and henceforth.

The graphical outputs show successful boundary mapping of chromosome images using DCT based GVF Active Contours.

VALIDATION OF CHARACTERIZATION EXPERIMENTS

In order to quantify the performance of a segmentation method, validation experiments are necessary. Validation is typically performed using one or two different types of truth models. In this work, ground truth model is not available and hence validation is performed on ordinal or ranking scale and then quantified. A set of 10 random samples is taken and characterization of each parameter is done. The outputs were tabulated in ranking order with "1" describing the best quality output and as the quality decreases the rank increases up to rank "97". Rank "98" is a special case, where the output image is rejected based on quality or the output image is not available due to numerical instability possibly caused due to the greater number of contour points[5]. The tables represent characterization studies for each parameter.

Each table denotes variation for only one parameter either between the lower and upper limits of the parameter or between the lower and upper limits giving significantly different output, with the other parameters taking a constant value. Hence, the best parameter value of that table is the one that gives maximum good quality outputs for all samples or a majority of samples, and exhaustive study on every parameter is done by treating the other parameters as constants.

The statistical median is used to judge the distribution of values for each parameter value for all samples. When the median leans towards the lower values, i.e., towards "1", it indicates that almost 50% of the outputs lean towards "1", making that particular parameter value an optimal one and that optimal value is chosen. The characterization studies reveal that each parameter sometimes has an optimal range within which it can assume any value thereby giving majority good outputs for all samples. But for the sake of experimental purposes, only the investigated discrete value of each parameter that gave best output was chosen. An important point to be noted is that characterization studies have been performed for those parameter values which give either significant output or significant difference in performance between adjacent parameter values. Those parameter values where there is no significant difference between adjacent parameter values have not been tabulated. Also, those parameter values outside the tabulated range which gave no proper results have not been tabulated.

Table.1 Characterization of Sigma

Sample No.	GVF (DCT) s									
	0.05	0.1	0.15	0.2	**0.25**	0.5	0.6	0.8	1	1.2
1	77	77	77	77	**77**	29	77	29	13	77
2	77	77	77	29	**13**	13	13	13	29	77
3	97	77	34	29	**77**	29	78	81	75	78
4	77	77	29	29	**31**	70	79	79	79	78
5	97	97	97	97	**98**	98	98	98	98	98
6	86	86	46	38	**38**	14	38	38	46	78
7	97	97	97	97	**98**	98	98	98	98	98
8	86	86	86	54	**98**	98	98	98	98	98
9	77	77	77	77	**38**	46	15	77	13	79
10	86	77	13	77	**46**	65	78	13	78	77
Median	86	77	77	**66**	**62**	**55**	78	78	77	78

In Table 1, the median indicates that the acceptable optimal range of s is 0.2 to 0.5. The best value compared qualitatively amongst those tested is 0.25 and hence it is chosen for performing further characterization.

Table 2. Characterization of Mu

Sample No.	GVF (DCT) µ					
	0.05	**0.075**	0.09375	0.1125	0.15	0.3
1	23	**21**	21	23	23	97
2	21	**5**	23	23	23	97
3	30	**29**	29	46	50	97
4	23	**23**	23	40	23	97
5	98	**98**	98	97	97	97
6	48	**40**	48	48	46	97
7	98	**98**	50	50	34	97
8	98	**89**	62	97	97	97
9	71	**86**	30	71	71	97
10	23	**21**	29	71	23	97
Median	**39**	**35**	**29**	49	40	97

In Table 2, the median indicates that the acceptable optimal range of µ is 0.05 to 0.09375. The best value compared qualitatively amongst those tested is 0.075 and hence it is chosen for performing further characterization.

Table 3. Characterization of Alpha

Sample No.	GVF (DCT) a				
	0	0.125	0.25	0.5	1
1	**7**	23	77	71	77
2	**7**	30	29	77	30
3	**5**	67	78	78	67
4	**23**	23	79	80	80
5	**98**	98	98	98	97
6	**98**	48	40	46	87
7	**98**	98	98	97	97
8	**90**	86	62	97	94
9	**21**	23	23	71	27
10	**5**	7	23	21	71
Median	**22**	**39**	70	78	79

In Table 3, the median indicates that the acceptable optimal range of a extends from 0 to 0.125. The best value compared qualitatively amongst those tested is 0 and hence it is chosen for performing further characterization.

Table 4. Characterization of Beta

Sample No.	GVF (DCT) ß		
	0	0.5	1
1	**23**	30	71
2	**5**	21	21
3	**5**	21	31
4	**21**	23	71
5	**98**	98	98
6	**98**	46	70
7	**98**	98	98
8	**38**	94	13
9	**23**	71	71
10	**3**	21	30
Median	**23**	**38**	71

In Table 4, the median indicates that the acceptable optimal range of ß extends from 0 to 0.5. The best value compared qualitatively amongst those tested is 0 and hence it is chosen for performing further characterization.

Table 5. Characterization of Kappa

Sample No.	GVF (DCT) ?					
	0	0.5	**0.625**	0.75	0.875	1
1	97	7	**5**	5	5	5
2	97	3	**3**	3	1	1
3	97	21	**19**	21	30	67
4	97	7	**7**	7	23	71
5	97	98	**98**	98	98	98
6	97	98	**98**	98	86	98
7	97	98	**98**	98	98	98
8	97	86	**98**	97	98	82
9	97	7	**7**	23	23	21
10	97	21	**5**	19	19	21
Median	97	**21**	**13**	**22**	**26**	69

In Table 5, the median indicates that the acceptable optimal range of ? extends from 0.5 to 0.875. The best value compared qualitatively amongst those tested is 0.625.

Hence the optimal set of parameter values that give good boundary mapping for the given class of chromosome images is s = 0.25, µ = 0.075, a = 0, ß = 0, and ? = 0.625. A safe limit of 5% tolerance can be introduced to the optimal range of parameter values to make them suitable for use in similar classes of chromosome spread images (indicated in Table 6).

Table 6. Optimal range of DCT based GVF Active Contour parameter values for tested chromosome spread images

Parameter	Parameter Value used for tested spread image	Acceptable Range of Parameter values	Acceptable Range of Values at 5% tolerance
GVF (DCT) s	0.25	[0.2 , 0.5]	[0.1900 , 0.5250]
GVF (DCT) µ	0.075	[0.05 , 0.09375]	[0.0475 , 0.0984]
GVF (DCT) a	0	[0 , 0.125]	[0.0000 , 0.1313]
GVF (DCT) ß	0	[0 , 0.5]	[0.0000 , 0.5250]
GVF (DCT) ?	0.625	[0.5 , 0.875]	[0.4750 , 0.9187]

STATISTICAL VALIDATION OF CHARACTERIZATION EXPERIMENTS

The parameters act independently on the boundary mapping scheme. In each characterization, the effect of other parameters will also be felt as they assume a definite constant value. In the course of the characterization study from Table 1 to Table 5, optimum values for the respective parameters are chosen and applied as constant in the characterization study of the next parameter in the successive table. In the last characterization study shown in Table 5, the values of s, µ, a and ß take on the chosen optimal values and only ? is investigated, thereby yielding a one way variation. Hence, one way analysis of variance on Table 5 is sufficient to test the significance of the entire boundary mapping process. A significant outcome from Table 5 will justify that the experimental results of Table 5 are valid, implying that the selected parameter values from Table 1 to Table 4 used as constants in Table 5 are also valid.

Hence, one way Anova test is performed on the last characterization (Table 5) to judge the experimental results. At the customary .05 significance level, one way Anova test yields a p value of 7.17082E-08 on Table 5, which rejects the null hypothesis. The very small p-value of 7.17082E-08 indicates that differences between the column means are highly significant. The probability of this outcome under the null hypothesis is less than 8 in 100,000,000. The test therefore strongly supports the alternate hypothesis that one or more of the samples are drawn from populations with different means. This implies that the results in Table 5 do not arise out of mere fluctuations and that the results are actually significant. Therefore the experimental results are valid. This justifies that a suitable value of parameter ? can be chosen from Table 5, and that the constant values of parameters s, µ, a, and ß used in Table 5 are also valid as these values also have significant influence on the results tabulated in Table 5. Therefore, the experimental results and the inferences are also significant.

STANDARDIZATION

Characterization studies have yielded an acceptable optimal range of values for the parameters s,µ,a,ß and ?. To establish that the parameter values are standardized with reference to similar classes of chromosome spread images, standardization experiments are carried out in a similar class of chromosome spread images from a different dataset, made available by the kind courtesy of Dr.Michael Difilippantonio, Staff Scientist at the Section of Cancer Genomics, Genetics Branch/CCR/NCI/NIH, Bethesda MD.

The same characterized parameter values of s = 0.25, µ = 0.075, a = 0, ß = 0, and ? = 0.625 have been used. Good boundary mapping results have been obtained and the results are shown in the following pages. Each sample is unique as the chromosomes are imaged in a fluid medium, and random bending effects are manifested. Hence it is shown that the DCT based GVF Active Contour, governed by the characterized values of the parameters of s = 0.25, µ = 0.075, a = 0, ß = 0, and ? = 0.625 are able to overcome the variations in the shape of the chromosomes and give good boundary mapping in each of the samples.

A few samples are illustrated in the following pages. The chromosome image is seen in gray scale, while the DCT based GVF Active Contour mapped boundary is shown in red.

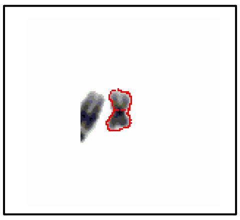
Fig.7 Sample1


Fig.8 Sample2

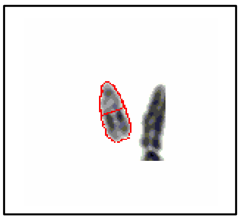
Fig.9 Sample3

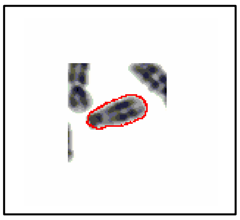
Fig.10 Sample4

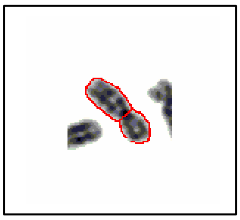
Fig.11 Sample5


Fig.12 Sample6

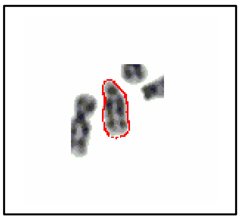
Fig.13 Sample7

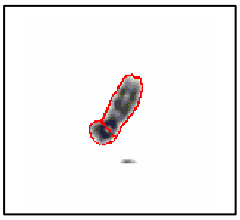
Fig.14 Sample8

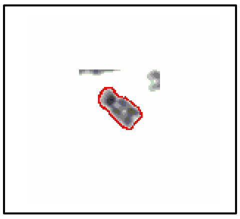
Fig.15 Sample9

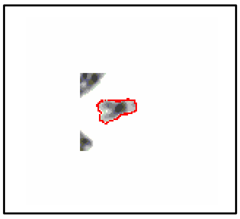
Fig.16 Sample10

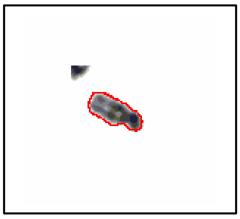
Fig.17 Sample11


Fig.18 Sample12


Fig.19 Sample13

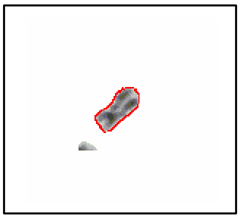
Fig.20 Sample14

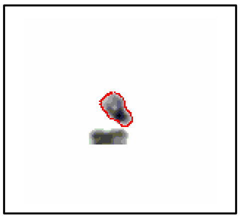
Fig.21 Sample15

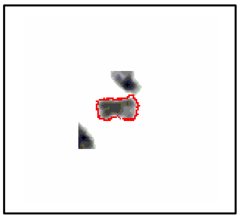
Fig.22 Sample16

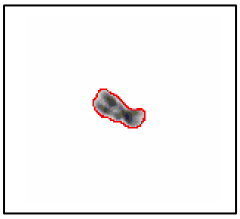
Fig.23 Sample17

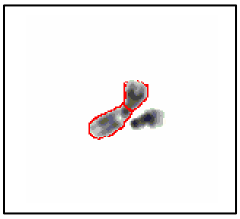
Fig.24 Sample18


Fig.25 Sample19

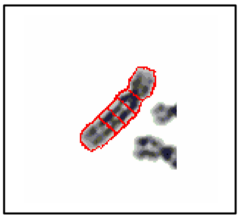
Fig.26 Sample20

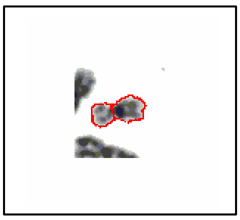
Fig.27 Sample21

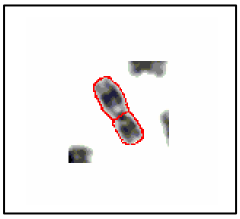
Fig.28 Sample22

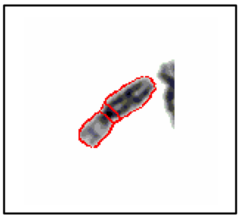
Fig.29 Sample23

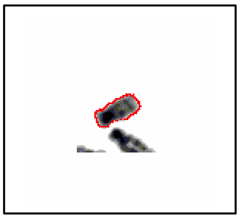
Fig.30 Sample24

From the above illustrations of boundary mapped chromosomes, it is inferred that the set of parameter values s = 0.25, μ = 0.075, a = 0, ß = 0, and ? = 0.625 governing the formulation of the DCT based GVF Active Contours are hence standardized.

EVALUATION OF STANDARDIZATION

To assess the success of the standardization, the DCT based GVF Active Contours with the same characterized values of the parameters were applied to boundary map chromosome spread images from a different dataset, which was made available by the kind courtesy of Prof.Ekaterina Detcheva, at the Artificial Intelligence Department, Institute of Mathematics and Informatics, Sofia, Bulgaria.

A few graphical results are presented subsequently, which indicate that the standardization has been successful. The chromosome is shown in gray scale and the mapped boundary is indicated in red color.

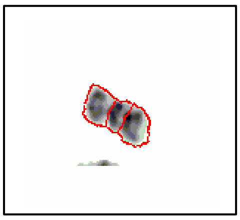
Fig.31 Sample 1

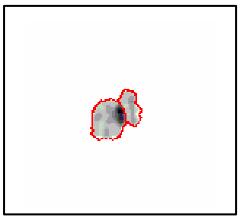
Fig.32 Sample 2

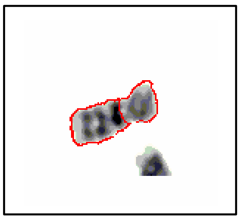
Fig.33 Sample 3

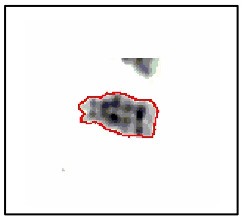
Fig.34 Sample 4

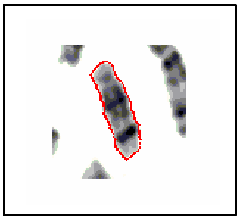
Fig.35 Sample 5

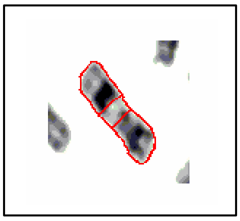
Fig.36 Sample 6

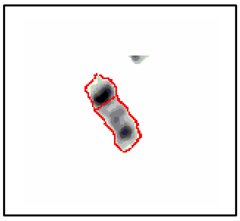
Fig.37 Sample 7

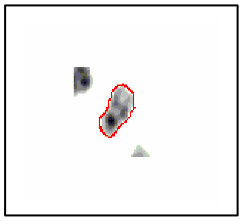
Fig.38 Sample 8

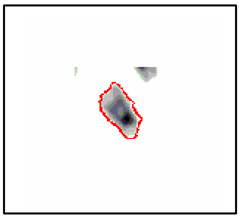
Fig.39 Sample 9

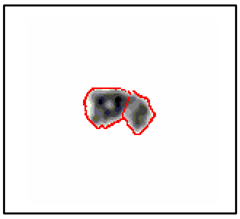
Fig.40 Sample 10

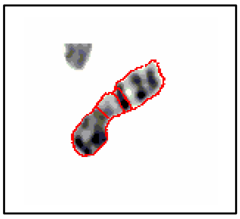
Fig.41 Sample 11

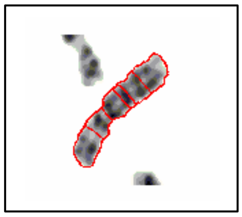
Fig.42 Sample 12

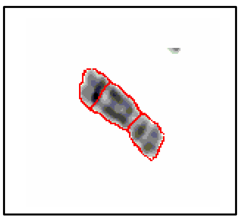
Fig.43 Sample 13

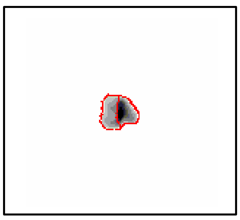
Fig.44 Sample 14

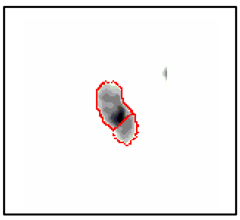
Fig.45 Sample 15

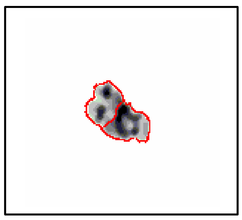
Fig.46 Sample 16

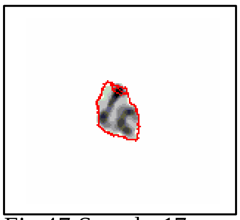

Fig.47 Sample 17

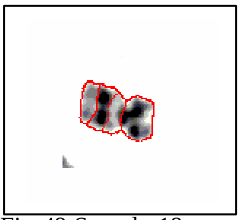

Fig.48 Sample 18

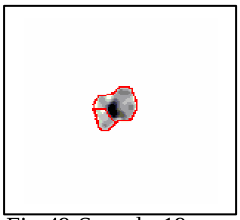

Fig.49 Sample 19

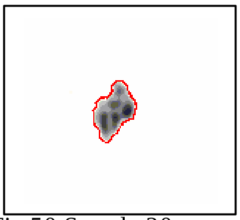

Fig.50 Sample 20

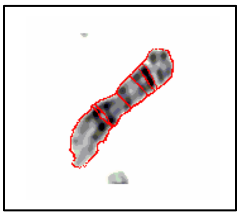

Fig.51 Sample 21

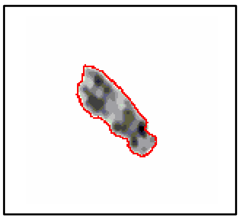

Fig.52 Sample 22

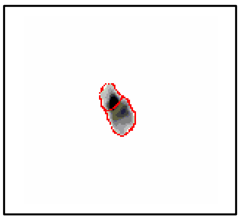

Fig.53 Sample 23

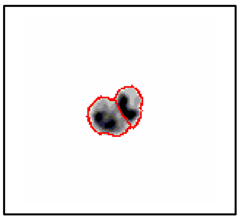

Fig.54 Sample 24

ERROR QUANTIFICATION

Error Quantification is done to assess the experimental results. The error in Boundary Mapping is measured as a difference between axial radius of the original chromosome image sample and the axial radius of the boundary mapped chromosome image sample. The error in boundary mapping for the samples used for characterization is shown in Table 7.

Table 7. Error in Boundary Mapping for sample images used for characterization

Sample No.	**Original Image Major Axis Radius (pixels)**	**Contour Image Major Axis Radius (pixels)**	**Major Axis Error (Original - Contour) (pixels)**	**Major Axis Absolute Error abs(Original - Contour) (pixels)**	**Original Image Minor Axis Radius (pixels)**	**Contour Image Minor Axis Radius (pixels)**	**Minor Axis Error (Original - Contour) (pixels)**	**Minor Axis Absolute Error abs(Original - Contour) (pixels)**
1	19.836534	20.614610	-0.778076	0.778076	7.654679	8.154604	-0.499926	0.499926
2	15.531852	15.888311	-0.356459	0.356459	7.348310	7.831433	-0.483123	0.483123
3	19.450454	20.106271	-0.655817	0.655817	7.748832	8.179759	-0.430927	0.430927
4	35.059325	35.516327	-0.457002	0.457002	8.620817	9.395544	-0.774727	0.774727
5	28.890790	29.151164	-0.260374	0.260374	7.735980	8.187389	-0.451409	0.451409
6	18.082140	18.692496	-0.610356	0.610356	7.470833	7.792613	-0.321780	0.321780
7	26.226850	26.181850	0.045000	0.045000	6.625715	7.047331	-0.421616	0.421616
8	26.033162	26.489206	-0.456044	0.456044	7.697243	8.131959	-0.434716	0.434716
9	20.525006	21.179205	-0.654199	0.654199	8.725828	9.510494	-0.784667	0.784667
10	27.247951	27.158149	0.089802	0.089802	6.839096	7.067086	-0.227990	0.227990
11	15.903326	15.845969	0.057357	0.057357	7.782958	8.142976	-0.360018	0.360018
12	27.435787	27.275522	0.160265	0.160265	8.315512	8.523697	-0.208185	0.208185
Max Absolute Error				**0.778076**				**0.784667**
Min Absolute Error				**0.045000**				**0.208185**

The maximum absolute error from Table7 is **0.784667** pixel and the minimum absolute error is **0.045000** pixel. The contour is one pixel thick. The initial contour converges to the boundary in step sizes of one pixel. Considering the above two facts, it is quite logical that there could be an error approximating one pixel. Since the errors given by Table7 are less than one pixel, the boundary mapping obtained can be accepted as accurate. This justifies that the parameter values s = 0.25, µ = 0.075, a = 0, ß = 0, and ? = 0.625 that have been used for boundary mapping using DCT based GVF Active Contours can be accepted as characterized values for similar classes of chromosome spread images. The error in boundary mapping for the samples used for standardization is shown in Table 8.

Table 8. Error in Boundary Mapping for sample images used for standardization

Sample No.	Original Image Major Axis Radius (pixels)	Contour Image Major Axis Radius (pixels)	Major Axis Error (Original - Contour) (pixels)	Major Axis Absolute Error (Original - Contour) (pixels)	Original Image Minor Axis Radius (pixels)	Contour Image Minor Axis Radius (pixels)	Minor Axis Error (Original - Contour) (pixels)	Minor Axis Absolute Error (Original - Contour) (pixels)
1	15.671966	16.664304	-0.992338	0.992338	8.632178	9.408042	-0.775864	0.775864
2	27.532960	28.455320	-0.922360	0.922360	9.363175	10.831798	-1.468623	1.468623
3	21.352938	22.573477	-1.220539	1.220539	9.245948	10.668792	-1.422845	1.422845
4	22.487728	22.988902	-0.501174	0.501174	9.487592	11.011601	-1.524009	1.524009
5	30.832858	31.631947	-0.799089	0.799089	9.916949	11.222596	-1.305647	1.305647
6	26.527726	27.749187	-1.221461	1.221461	10.348389	11.772646	-1.424257	1.424257
7	20.421685	22.022552	-1.600867	1.600867	9.300520	10.527103	-1.226584	1.226584
8	28.932339	30.032657	-1.100319	1.100319	9.705534	11.185087	-1.479554	1.479554
9	17.361945	18.709701	-1.347756	1.347756	8.734208	10.217936	-1.483728	1.483728
10	14.592386	15.831201	-1.238815	1.238815	7.461672	8.903638	-1.441966	1.441966
11	21.530209	22.035274	-0.505066	0.505066	8.816231	10.256872	-1.440641	1.440641
12	18.516333	19.480915	-0.964582	0.964582	7.394475	8.839323	-1.444848	1.444848
13	21.980379	22.722356	-0.741977	0.741977	8.888960	10.173 608	-1.284649	1.284649
14	19.394772	20.504988	-1.110216	1.110216	8.444747	9.892300	-1.447553	1.447553
15	13.283334	14.830840	-1.547507	1.547507	7.783275	8.997038	-1.213763	1.213763
16	15.758397	16.832960	-1.074563	1.074563	8.689258	9.750896	-1.061639	1.061639
17	20.383368	21.569564	-1.186196	1.186196	8.731019	10.135830	-1.404811	1.404811
18	29.016552	29.744011	-0.727460	0.727460	8.824018	10.088889	-1.264871	1.264871
19	20.328609	21.203247	-0.874638	0.874638	8.570169	9.562535	-0.992366	0.992366
20	38.396106	39.384758	-0.988652	0.988652	9.930610	11.533310	-1.602701	1.602701
21	20.593760	21.963540	-1.369780	1.369780	8.777635	10.172417	-1.394782	1.394782
22	28.014880	29.189257	-1.174377	1.174377	9.106209	10.659509	-1.553300	1.553300
23	35.057991	36.212418	-1.154428	1.154428	9.554718	11.220442	-1.665724	1.665724
24	17.289731	18.370185	-1.080455	1.080455	8.024122	9.004566	-0.980445	0.980445
25	22.021634	22.461027	-0.439393	0.439393	8.142623	9.489822	-1.347199	1.347199
26	29.784084	30.682099	-0.898015	0.898015	9.548830	10.755476	-1.206646	1.206646
27	33.294617	34.134478	-0.839861	0.839861	9.542091	11.054903	-1.512812	1.512812
28	24.728291	25.920548	-1.192257	1.192257	9.318735	10.594356	-1.275622	1.275622
29	15.355989	16.272398	-0.916409	0.916409	7.927053	9.153714	-1.226661	1.226661
30	15.797688	16.992960	-1.195272	1.195272	8.164426	9.377414	-1.212988	1.212988
31	19.119752	20.198432	-1.078680	1.078680	8.006951	9.386859	-1.379909	1.379909
32	50.529747	51.836646	-1.306899	1.306899	9.569420	11.155712	-1.586292	1.586292
33	28.677206	29.719430	-1.042224	1.042224	9.347141	10.847365	-1.500224	1.500224
34	18.489779	19.566706	-1.076928	1.076928	9.020151	10.322819	-1.302668	1.302668
35	15.369255	16.562642	-1.193387	1.193387	8.009787	9.352062	-1.342275	1.342275
36	22.002596	22.199599	-0.197003	0.197003	8.269518	9.260998	-0.991480	0.991480
37	22.856044	23.861794	-1.005750	1.005750	8.909892	10.293682	-1.383790	1.383790
38	18.296507	19.566748	-1.270241	1.270241	9.445701	10.707874	-1.262173	1.262173
39	27.960635	29.151157	-1.190522	1.190522	8.545565	10.136476	-1.590911	1.590911
40	18.852903	20.423583	-1.570681	1.570681	8.455191	9.796682	-1.341491	1.341491
41	22.698254	22.763508	-0.065254	0.065254	8.464508	9.752790	-1.288282	1.288282
42	12.293282	13.703855	-1.410574	1.410574	7.320788	8.823351	-1.502564	1.502564

43	11.489264	12.447829	-0.958566	0.958566	7.235781	8.566689	-1.330908	1.330908
44	18.432328	19.577044	-1.144716	1.144716	7.436791	9.010851	-1.574060	1.574060
45	12.968119	14.117667	-1.149548	1.149548	7.803107	8.611738	-0.808631	0.808631
46	14.282209	15.730363	-1.448154	1.448154	7.647730	8.570545	-0.922816	0.922816
47	19.454318	20.187653	-0.733335	0.733335	7.421526	8.633051	-1.211525	1.211525
48	20.625064	21.377546	-0.752482	0.752482	8.360867	9.469176	-1.108310	1.108310
49	24.934309	25.765914	-0.831605	0.831605	9.539810	10.676653	-1.136843	1.136843
50	20.374887	21.820383	-1.445496	1.445496	8.790606	9.990901	-1.200295	1.200295
51	19.383527	19.820843	-0.437316	0.437316	8.478031	9.419203	-0.941172	0.941172
52	19.327516	20.508350	-1.180835	1.180835	8.350576	9.233636	-0.883060	0.883060
53	26.433113	27.533623	-1.100511	1.100511	8.610975	9.593304	-0.982329	0.982329
54	12.101642	12.949808	-0.848166	0.848166	7.246340	8.059449	-0.813109	0.813109
55	16.634324	17.486275	-0.851951	0.851951	8.394216	9.252824	-0.858608	0.858608
56	14.749573	16.175581	-1.426008	1.426008	6.833781	8.201446	-1.367665	1.367665
57	26.644550	27.732467	-1.087917	1.087917	9.192708	10.450890	-1.258182	1.258182
58	46.708148	47.716019	-1.007871	1.007871	9.854564	11.425238	-1.570674	1.570674
59	11.804992	12.946824	-1.141832	1.141832	6.838070	8.085564	-1.247494	1.247494
60	14.789925	15.845047	-1.055122	1.055122	8.045290	9.278818	-1.233528	1.233528
61	16.053096	17.098621	-1.045525	1.045525	8.571831	10.044725	-1.472894	1.472894
62	16.381754	17.627738	-1.245984	1.245984	8.109770	9.287800	-1.178031	1.178031
63	24.880002	26.125909	-1.245907	1.245907	8.112620	9.060594	-0.947974	0.947974
64	23.946641	25.039662	-1.093021	1.093021	12.670524	13.276545	-0.606021	0.606021
65	12.162489	13.637709	-1.475220	1.475220	8.477049	9.129125	-0.652076	0.652076
66	29.266172	30.914282	-1.648110	1.648110	10.406857	11.619620	-1.212763	1.212763
67	14.633115	15.986863	-1.353749	1.353749	7.746963	8.767422	-1.020460	1.020460
68	41.377986	42.913452	-1.535466	1.535466	8.388075	9.731649	-1.343574	1.343574
69	30.902650	31.722539	-0.819889	0.819889	7.790671	9.171754	-1.381083	1.381083
70	30.486127	32.010595	-1.524468	1.524468	7.433136	8.958509	-1.525374	1.525374
71	53.003739	54.121765	-1.118025	1.118025	9.009000	10.065934	-1.056934	1.056934
72	23.914936	25.087823	-1.172888	1.172888	8.439396	9.522967	-1.083572	1.083572
73	25.988345	27.436165	-1.447820	1.447820	7.605870	9.074429	-1.468560	1.468560
74	15.201740	16.600042	-1.398303	1.398303	10.073521	10.899285	-0.825764	0.825764
75	27.651519	28.806415	-1.154896	1.154896	9.832643	11.599894	-1.767251	1.767251
76	18.248415	19.923112	-1.674697	1.674697	8.730340	10.555582	-1.825242	1.825242
77	27.280692	28.092240	-0.811548	0.811548	10.746050	12.236822	-1.490772	1.490772
78	31.649805	32.705289	-1.055484	1.055484	12.474942	13.596004	-1.121062	1.121062
79	33.039166	34.504250	-1.465084	1.465084	10.738993	12.331706	-1.592714	1.592714
80	37.867089	38.796924	-0.929835	0.929835	12.673802	14.121217	-1.447415	1.447415
81	35.310917	36.485378	-1.174461	1.174461	10.736892	12.151016	-1.414124	1.414124
82	27.148531	28.467029	-1.318498	1.318498	9.832887	11.683787	-1.850900	1.850900
83	31.084442	32.367469	-1.283027	1.283027	10.187646	12.011337	-1.823691	1.823691
84	30.275702	31.981141	-1.705439	1.705439	10.312149	12.115291	-1.803142	1.803142
85	38.721848	39.850035	-1.128187	1.128187	10.463738	12.253172	-1.789434	1.789434
86	38.172823	39.479579	-1.306756	1.306756	10.713896	12.524580	-1.810684	1.810684
87	22.174872	23.861436	-1.686564	1.686564	9.386474	11.147687	-1.761213	1.761213
88	25.306473	26.855064	-1.548591	1.548591	9.580741	11.419127	-1.838386	1.838386
89	13.389388	15.173893	-1.784505	1.784505	8.709630	10.128332	-1.418702	1.418702
90	27.699672	29.201280	-1.501609	1.501609	10.024375	11.586792	-1.562417	1.562417
91	18.674080	20.424525	-1.750446	1.750446	8.942478	10.632208	-1.689731	1.689731
92	15.202306	16.916676	-1.714370	1.714370	8.345341	9.837005	-1.491664	1.491664
93	18.159180	19.451072	-1.291892	1.291892	7.885159	9.496574	-1.611415	1.611415
94	17.823696	18.939046	-1.115350	1.115350	7.968971	9.407034	-1.438064	1.438064
95	20.392552	21.559613	-1.167061	1.167061	8.803825	9.650425	-0.846600	0.846600
96	16.053326	16.403345	-0.350020	0.350020	8.705797	9.974861	-1.269065	1.269065
97	28.417059	30.076832	-1.659774	1.659774	8.315611	9.761672	-1.446062	1.446062

98	26.279791	27.604151	-1.324360	1.324360	8.767107	10.210356	-1.443249	1.443249
99	24.855239	25.694758	-0.839520	0.839520	9.260129	10.562985	-1.302856	1.302856
100	27.056032	28.519464	-1.463432	1.463432	8.756193	10.247444	-1.491251	1.491251
101	12.497205	13.844260	-1.347055	1.347055	7.789650	9.230230	-1.440580	1.440580
102	25.701113	26.474269	-0.773156	0.773156	17.143213	18.078908	-0.935695	0.935695
103	21.610747	22.533912	-0.923166	0.923166	9.019719	10.454644	-1.434925	1.434925
104	21.698508	22.527944	-0.829436	0.829436	7.757083	9.282188	-1.525105	1.525105
105	29.240446	30.331768	-1.091322	1.091322	17.788404	19.032339	-1.243935	1.243935
106	25.920061	27.632335	-1.712274	1.712274	8.251795	9.510343	-1.258548	1.258548
107	24.771901	25.425744	-0.653843	0.653843	8.477681	9.727825	-1.250144	1.250144
108	16.780813	17.776323	-0.995510	0.995510	6.505608	7.941176	-1.435568	1.435568
109	16.917350	18.471045	-1.553695	1.553695	7.064605	8.188661	-1.124056	1.124056
110	20.503965	21.762127	-1.258162	1.258162	7.975524	9.572154	-1.596631	1.596631
111	20.406026	21.803039	-1.397013	1.397013	8.998619	10.572175	-1.573557	1.573557
112	38.056659	39.396801	-1.340142	1.340142	8.009457	9.616864	-1.607407	1.607407
113	39.580016	40.758886	-1.178870	1.178870	10.498883	12.078433	-1.579550	1.579550
114	17.783921	19.247613	-1.463692	1.463692	7.437665	9.291699	-1.854034	1.854034
115	24.896309	26.735280	-1.838972	1.838972	9.673694	10.831072	-1.157378	1.157378
116	22.485539	24.034059	-1.548520	1.548520	9.022670	10.667461	-1.644791	1.644791
117	15.498861	16.578002	-1.079141	1.079141	8.037118	9.824751	-1.787633	1.787633
118	16.454983	17.499296	-1.044313	1.044313	9.140502	10.512071	-1.371569	1.371569
119	24.187462	25.000171	-0.812709	0.812709	9.623745	11.364589	-1.740844	1.740844
120	21.517824	22.983501	-1.465677	1.465677	8.703217	9.981869	-1.278652	1.278652
121	15.098594	16.257515	-1.158921	1.158921	9.038787	10.489106	-1.450319	1.450319
122	14.129186	15.727674	-1.598489	1.598489	7.418632	9.046995	-1.628363	1.628363
123	20.764022	22.197016	-1.432994	1.432994	8.768812	10.303772	-1.534960	1.534960
124	18.188267	19.592789	-1.404522	1.404522	8.382052	10.039192	-1.657140	1.657140
125	18.939243	20.285314	-1.346072	1.346072	7.481623	9.264128	-1.782505	1.782505
126	19.844294	21.208168	-1.363875	1.363875	8.230198	9.884893	-1.654695	1.654695
127	26.238065	27.533841	-1.295777	1.295777	9.234557	10.794933	-1.560376	1.560376
128	50.861033	52.615955	-1.754922	1.754922	8.889528	10.382229	-1.492702	1.492702
129	16.336610	16.855539	-0.518929	0.518929	9.577288	10.602798	-1.025510	1.025510
130	13.429074	14.955483	-1.526409	1.526409	8.009254	9.337699	-1.328446	1.328446
131	14.414971	15.399156	-0.984185	0.984185	6.849160	7.729817	-0.880658	0.880658
132	47.911167	49.169514	-1.258347	1.258347	9.726675	11.354186	-1.627511	1.627511
133	38.805225	40.123353	-1.318128	1.318128	11.598487	12.881671	-1.283184	1.283184
134	13.348832	14.576388	-1.227557	1.227557	7.683565	9.474765	-1.791200	1.791200
135	38.432549	39.831625	-1.399076	1.399076	11.024138	12.658246	-1.634108	1.634108
136	20.330862	21.838440	-1.507578	1.507578	8.690759	10.385698	-1.694940	1.694940
137	15.077049	16.698517	-1.621468	1.621468	8.835773	10.639860	-1.804087	1.804087
138	26.989340	28.234650	-1.245310	1.245310	9.409284	11.118903	-1.709619	1.709619
139	17.889180	19.312198	-1.423018	1.423018	8.118620	9.788408	-1.669788	1.669788
140	28.259209	30.067447	-1.808238	1.808238	9.498699	10.987069	-1.488371	1.488371
141	24.427379	25.823162	-1.395784	1.395784	9.695588	11.295594	-1.600006	1.600006
142	23.627306	25.091738	-1.464432	1.464432	8.095011	9.962331	-1.867320	1.867320
143	23.810684	25.061957	-1.251273	1.251273	9.419878	10.759572	-1.339695	1.339695
144	12.113925	13.343194	-1.229269	1.229269	8.018322	9.513394	-1.495073	1.495073
145	16.915286	18.386556	-1.471270	1.471270	7.838470	9.005787	-1.167317	1.167317
146	35.318252	36.090017	-0.771764	0.771764	9.118425	10.590449	-1.472024	1.472024
147	19.708705	21.229899	-1.521195	1.521195	9.374193	10.853156	-1.478963	1.478963
148	23.910337	25.694098	-1.783761	1.783761	9.459880	11.234284	-1.774405	1.774405
149	48.113620	49.349568	-1.235948	1.235948	10.490992	12.338561	-1.847570	1.847570
150	49.917137	51.202320	-1.285183	1.285183	9.082107	10.856781	-1.774674	1.774674
151	32.556208	34.235269	-1.679062	1.679062	9.462194	11.297245	-1.835052	1.835052
152	33.207234	34.848162	-1.640928	1.640928	8.691695	10.397784	-1.706090	1.706090

153	16.979062	18.520299	-1.541237	1.541237	6.946655	8.726264	-1.779609	1.779609
154	24.605822	25.482857	-0.877035	0.877035	8.113264	9.825922	-1.712658	1.712658
155	26.403204	27.969927	-1.566723	1.566723	9.176485	10.785247	-1.608762	1.608762
156	24.013608	25.615960	-1.602352	1.602352	9.101337	10.687972	-1.586636	1.586636
157	22.040457	23.670391	-1.629934	1.629934	8.236205	9.917901	-1.681697	1.681697
158	22.318277	23.708479	-1.390202	1.390202	8.551382	10.080071	-1.528689	1.528689
159	33.735806	35.040720	-1.304914	1.304914	13.508514	14.897244	-1.388730	1.388730
160	17.999605	19.458788	-1.459184	1.459184	8.339721	10.106280	-1.766559	1.766559
161	18.113859	19.327966	-1.214108	1.214108	8.989681	10.367453	-1.377772	1.377772
162	19.849320	21.163800	-1.314480	1.314480	9.221759	10.885869	-1.664110	1.664110
163	25.485283	27.115437	-1.630155	1.630155	9.809878	11.182578	-1.372700	1.372700
164	19.018617	20.384091	-1.365475	1.365475	8.855341	10.276901	-1.421560	1.421560
165	21.826682	23.528871	-1.702189	1.702189	8.208094	9.807279	-1.599185	1.599185
166	34.173116	35.592430	-1.419314	1.419314	8.999310	10.646353	-1.647043	1.647043
167	24.058980	25.714750	-1.655770	1.655770	9.221398	10.775454	-1.554056	1.554056
168	24.626540	25.681728	-1.055188	1.055188	9.439789	11.080068	-1.640279	1.640279
169	23.730327	25.340916	-1.610589	1.610589	10.198267	11.521470	-1.323203	1.323203
170	23.158896	24.634195	-1.475299	1.475299	10.883928	12.350592	-1.466665	1.466665
171	26.493227	28.114194	-1.620967	1.620967	9.648455	11.410448	-1.761993	1.761993
172	30.716575	32.219983	-1.503408	1.503408	10.645538	12.154495	-1.508958	1.508958
173	38.913883	40.137957	-1.224074	1.224074	12.797589	14.295206	-1.497617	1.497617
174	20.061951	21.550700	-1.488749	1.488749	10.003156	11.760108	-1.756952	1.756952
175	13.854563	15.386945	-1.532382	1.532382	7.296950	9.041869	-1.744920	1.744920
176	23.742697	25.115406	-1.372709	1.372709	8.768824	10.567965	-1.799141	1.799141
177	20.425829	21.755126	-1.329297	1.329297	9.336815	10.901881	-1.565067	1.565067
178	29.062003	30.442511	-1.380508	1.380508	11.450939	12.834778	-1.383839	1.383839
179	19.064699	20.831931	-1.767232	1.767232	9.247087	10.903589	-1.656502	1.656502
180	36.065833	37.091060	-1.025227	1.025227	9.968086	11.696727	-1.728641	1.728641
181	15.063413	16.603463	-1.540050	1.540050	9.310657	10.967043	-1.656387	1.656387
182	20.179458	21.908645	-1.729187	1.729187	9.639445	10.791829	-1.152385	1.152385
183	16.231509	17.435943	-1.204434	1.204434	9.008868	10.525497	-1.516629	1.516629
184	19.017858	20.017165	-0.999306	0.999306	9.124801	10.912622	-1.787821	1.787821
185	25.782715	27.084142	-1.301427	1.301427	9.268583	10.984868	-1.716286	1.716286
186	13.096746	14.716790	-1.620044	1.620044	7.377308	8.988964	-1.611656	1.611656
187	18.901107	20.512836	-1.611729	1.611729	9.045009	10.747767	-1.702758	1.702758
188	26.622150	27.564319	-0.942169	0.942169	10.108389	11.481676	-1.373288	1.373288
189	27.987962	29.566069	-1.578107	1.578107	10.215272	11.776568	-1.561296	1.561296
190	30.533699	31.797310	-1.263612	1.263612	10.703308	12.138193	-1.434885	1.434885
191	16.565674	17.855143	-1.289469	1.289469	10.681040	12.164285	-1.483246	1.483246
192	15.178607	16.736527	-1.557920	1.557920	8.807469	10.605921	-1.798453	1.798453
193	21.685394	22.890356	-1.204962	1.204962	10.337343	11.604640	-1.267298	1.267298
194	19.167518	20.627483	-1.459965	1.459965	8.483991	10.266008	-1.782017	1.782017
195	34.836081	36.320664	-1.484583	1.484583	9.205800	10.976978	-1.771178	1.771178
196	16.695816	17.754742	-1.058926	1.058926	8.648719	10.009237	-1.360518	1.360518
197	19.529966	21.077051	-1.547085	1.547085	8.358981	10.112622	-1.753642	1.753642
198	27.355468	28.840489	-1.485021	1.485021	9.524901	11.259418	-1.734517	1.734517
199	20.233104	21.839734	-1.606630	1.606630	10.251424	11.689260	-1.437836	1.437836
200	23.975095	25.379406	-1.404311	1.404311	10.315971	11.819465	-1.503494	1.503494
201	31.430940	33.140342	-1.709402	1.709402	11.641736	13.443535	-1.801799	1.801799
202	17.028699	18.655821	-1.627122	1.627122	10.198261	11.846032	-1.647771	1.647771
203	25.219246	26.803637	-1.584391	1.584391	11.668128	13.193830	-1.525702	1.525702
204	23.708575	25.230878	-1.522303	1.522303	11.819731	13.367722	-1.547991	1.547991
205	30.280394	31.863098	-1.582705	1.582705	11.973341	13.718625	-1.745284	1.745284
206	29.584088	31.015642	-1.431554	1.431554	11.738661	13.559841	-1.821180	1.821180
207	13.561812	15.052638	-1.490827	1.490827	9.074158	10.651505	-1.577347	1.577347

208	23.363817	25.039424	-1.675608	1.675608	10.927165	12.728671	-1.801507	1.801507
209	17.912933	19.741272	-1.828339	1.828339	10.451326	11.800258	-1.348932	1.348932
210	29.972360	31.653878	-1.681518	1.681518	11.720213	13.179788	-1.459575	1.459575
211	23.772969	25.227189	-1.454220	1.454220	11.008461	12.518129	-1.509668	1.509668
212	23.439791	25.105427	-1.665636	1.665636	10.898287	12.468612	-1.570325	1.570325
213	17.124521	18.877162	-1.752641	1.752641	11.396605	12.910010	-1.513405	1.513405
214	28.736201	30.094898	-1.358698	1.358698	11.341097	12.790097	-1.449000	1.449000
215	31.470275	32.957390	-1.487115	1.487115	11.981835	13.617268	-1.635433	1.635433
216	18.778422	20.465092	-1.686671	1.686671	11.151816	12.424835	-1.273019	1.273019
217	18.425904	20.178760	-1.752856	1.752856	10.257129	11.906491	-1.649362	1.649362
218	22.580157	24.480231	-1.900074	1.900074	10.661173	12.341603	-1.680430	1.680430
Maximum Absolute Error				**1.900074**				**1.867320**
Minimum Absolute Error				**0.065254**				**0.606021**

The minimum absolute error is **0.065254** pixel, which justifies that the characterized parameter values s = 0.25, µ = 0.075, a = 0, ß = 0, and ? = 0.625 governing the formulation of the DCT based GVF Active Contours have been standardized, taking into account the earlier discussion regarding the one pixel width of the contour and one pixel step size. The minimum absolute error is a very low figure that defends that the characterized parameter values have been validated or standardized, and can be applied for boundary mapping similar classes of chromosome images.

However, the maximum absolute error is **1.900074** pixel, which is a little high. This can be explained as follows. In the standardization studies, concentration has not been applied on preprocessing applied to the chromosome image samples. Though a little preprocessing has been applied, still there has been residual background with a gray level very near to the intensity of the weak edge of the chromosome image sample, which can be easily visualized by the naked eye. This effect has contributed to an error in the convergence of the Active Contour which had mistaken the residual background as a weak edge, giving rise to more error. Since concentration on preprocessing techniques does not fall within the perspectives of this research work, only limited concentration has been applied and limited preprocessing has been done, which has given rise to this residual background effect near weak edges of chromosomes. Hence, it is suggested that preprocessing techniques may be suitably applied so that a little difference in gray level is introduced in background pixels near to weak edges of chromosomes, so that a distinction can be made in the gray level intensity between the background near the weak edges and the actual weak edges. This will bring down the maximum absolute error, and accurate boundary mapping can be obtained on all samples.

To assess the validity of the standardization experiments, error quantification has also been performed on the second dataset that has been used for evaluation of standardization. The error tabulation is shown in Table9.

Table 9. Error in Boundary Mapping for sample images used for evaluation of standardization

Sample No.	Original Image Major Axis Radius (pixels)	Contour Image Major Axis Radius (pixels)	Major Axis Error (Original - Contour) (pixels)	Major Axis Absolute Error (Original - Contour) (pixels)	Original Image Minor Axis Radius (pixels)	Contour Image Minor Axis Radius (pixels)	Minor Axis Error (Original - Contour) (pixels)	Minor Axis Absolute Error (Original - Contour) (pixels)
1	27.500278	29.252726	-1.752448	1.752448	13.225247	14.868594	-1.643347	1.643347
2	20.286862	21.439387	-1.152526	1.152526	13.044407	14.721727	-1.677320	1.677320
3	35.607997	37.318572	-1.710575	1.710575	13.381174	14.929574	-1.548400	1.548400
4	28.015593	29.788997	-1.773404	1.773404	13.907166	15.283898	-1.376732	1.376732
5	36.030472	37.719995	-1.689524	1.689524	10.313090	11.703343	-1.390253	1.390253
6	41.974266	43.250607	-1.276341	1.276341	11.818455	13.465882	-1.647427	1.647427
7	29.987934	31.354815	-1.366881	1.366881	10.379819	12.090108	-1.710289	1.710289
8	19.014212	20.279896	-1.265684	1.265684	8.960137	10.417969	-1.457832	1.457832

9	19.572380	21.253164	-1.680785	1.680785	10.368538	12.010517	-1.641979	1.641979
10	25.617336	27.225766	-1.608430	1.608430	14.244978	15.681151	-1.436173	1.436173
11	45.588463	46.599441	-1.010978	1.010978	12.200897	13.441862	-1.240965	1.240965
12	55.551831	56.730921	-1.179091	1.179091	12.096065	13.692535	-1.596470	1.596470
13	40.753298	41.902321	-1.149023	1.149023	12.244258	13.835217	-1.590960	1.590960
14	13.361401	15.098514	-1.737113	1.737113	12.139470	13.305029	-1.165559	1.165559
15	23.571876	24.927963	-1.356088	1.356088	10.399246	11.994666	-1.595420	1.595420
16	25.152889	26.959978	-1.807089	1.807089	14.673799	16.044380	-1.370582	1.370582
17	20.687946	22.150714	-1.462768	1.462768	13.681125	14.744788	-1.063663	1.063663
18	29.648501	30.682733	-1.034233	1.034233	16.339489	18.025519	-1.686030	1.686030
19	16.968261	18.401797	-1.433536	1.433536	12.399827	13.509598	-1.109771	1.109771
20	20.266691	21.948991	-1.682300	1.682300	12.440257	13.813558	-1.373301	1.373301
21	64.873797	65.902900	-1.029103	1.029103	13.721891	15.336432	-1.614541	1.614541
22	38.053659	39.289775	-1.236116	1.236116	13.300053	14.903674	-1.603621	1.603621
23	19.123143	20.186235	-1.063092	1.063092	9.400262	10.817705	-1.417443	1.417443
24	20.509131	21.892596	-1.383465	1.383465	14.591319	15.921873	-1.330554	1.330554
25	20.630242	22.593723	-1.963482	1.963482	13.357301	14.631125	-1.273824	1.273824
26	29.035200	30.363074	-1.327874	1.327874	10.781194	11.779053	-0.997859	0.997859
27	18.376779	19.535188	-1.158409	1.158409	11.275638	12.405822	-1.130184	1.130184
28	45.526893	46.683210	-1.156317	1.156317	10.990250	11.782551	-0.792302	0.792302
29	21.535536	22.157116	-0.621580	0.621580	9.449374	10.435725	-0.986350	0.986350
30	38.446929	38.351078	0.095851	0.095851	10.715210	11.803282	-1.088073	1.088073
31	35.836197	37.160304	-1.324107	1.324107	9.932954	11.041850	-1.108896	1.108896
32	30.869946	32.290574	-1.420628	1.420628	13.395228	14.085450	-0.690222	0.690222
33	21.417927	22.440844	-1.022918	1.022918	11.716527	13.232385	-1.515858	1.515858
34	62.497822	63.033789	-0.535967	0.535967	24.737276	25.821964	-1.084688	1.084688
35	18.154560	19.089820	-0.935260	0.935260	8.568300	9.926931	-1.358631	1.358631
36	26.217408	27.347200	-1.129792	1.129792	12.323615	13.652485	-1.328870	1.328870
37	35.806111	37.127095	-1.320984	1.320984	13.486754	14.883007	-1.396253	1.396253
38	31.916313	33.508124	-1.591811	1.591811	10.774331	12.401953	-1.627622	1.627622
39	32.668061	33.756079	-1.088018	1.088018	14.375519	16.046795	-1.671276	1.671276
40	22.413255	23.771220	-1.357965	1.357965	10.675502	12.436387	-1.760885	1.760885
41	19.480214	21.057702	-1.577488	1.577488	15.770160	16.646762	-0.876602	0.876602
42	38.955888	40.432240	-1.476353	1.476353	14.047309	15.710100	-1.662791	1.662791
43	63.876941	65.519154	-1.642213	1.642213	15.764328	17.368844	-1.604517	1.604517
44	24.307974	26.033315	-1.725341	1.725341	11.351497	12.995835	-1.644339	1.644339
45	19.800430	21.106789	-1.306360	1.306360	10.068588	11.336479	-1.267891	1.267891
46	31.409754	32.854170	-1.444416	1.444416	12.546744	13.895688	-1.348944	1.348944
47	29.162427	30.887020	-1.724593	1.724593	11.306874	12.757023	-1.450149	1.450149
48	48.068995	49.399138	-1.330143	1.330143	12.178446	13.463193	-1.284747	1.284747
49	22.282490	23.503758	-1.221269	1.221269	13.715583	15.211781	-1.496198	1.496198
50	23.494014	24.937220	-1.443207	1.443207	10.257538	11.756778	-1.499240	1.499240
Maximum Absolute Error				**1.963482**				**1.760885**
Minimum Absolute Error				**0.095851**				**0.690222**

It is found that the error varies between **0.095851** and **1.963482**, which is similar to the error measures obtained from the standardization experiments (discussed in previous paragraphs). Therefore, the same inferences that have been discussed earlier are valid. The very low of the minimum absolute error indicates the success of the boundary mapping scheme and the high value of the maximum absolute error justifies exploration of suitable preprocessing techniques

VII. CONCLUSION

The Discrete Cosine Transform based Gradient Vector Flow Active Contours can be used for successful efficient boundary mapping of chromosome spread images. The values s = 0.25, µ = 0.075, a = 0, ß = 0, and ? = 0.625 have hence been standardized and evaluated. Therefore, they can be used in DCT based GVF Active Contours for efficient boundary mapping of similar classes of chromosome spread images.

VIII. ACKNOWLEDGEMENT

The authors express their thanks to **Dr.Michael Difilippantonio**, *Staff Scientist at the Section of Cancer Genomics, Genetics Branch/CCR/NCI/ NIH, Bethesda MD*; **Prof.Ekaterina Detcheva** at the *Artificial Intelligence Department, Institute of Mathematics and Informatics, Sofia, Bulgaria*; **Prof.Ken Castleman** and **Prof.Qiang Wu**, from *Advanced Digital Imaging Research, Texas* for their help in providing chromosome spread images.

IX. REFERENCES

[1] McInerney T. and D. Terzopoulos, Deformable models in medical image analysis, IEEE Proceedings of the Workshop on Mathematical Methods in Biomedical Image Analysis. (1996) pp: 171-180

[2] Prabhu Britto A. and G.Ravindran, Boundary Mapping of Chromosome Images using Gradient Vector Flow Active Contours and Investigations, Academic Open Internet Journal (accepted) (2005)

[3] Prabhu Britto A. and G. Ravindran, Boundary mapping of chromosome spread images using optimal set of parameter values in Discrete Cosine Transform based Gradient Vector Flow Active Contours, J. Applied Sci. (Ansinet) (accepted) (2005)

[4] Kass M., A. Witkin, D. Terzopoulos, Snakes: active contour models, Int. J. Comp. Vision 1 (1987). pp: 321–331

[5] Rueckert D., Segmentation and tracking in cardiovascular MR images using geometrically deformable models and templates, PhD thesis, Imperial College of Science, Technology and Medicine, London (1997)

[6] C. Xu and J.L. Prince, "Gradient Vector Flow: A New External Force for Snakes", IEEE Proc. Conf. on Comp. Vis. Patt. Recog. (CVPR'97) 66-71

[7] Leroy B., I.Herlin and L.D.Cohen, Multi-resolution algorithms for active contour models, In 12^{th} Intl. Conf. on Analysis and Optimization of Systems. (1996) pp: 58-65

[8] Cohen L.D., On active contours and balloons, CVGIP: Image Understanding, 53(2). (1991) pp:211-218.

[9] Cohen L.D. and I.Cohen, Finite-element methods for active contour models and balloons for 2-D and 3-D images, IEEE Trans. On Pattern Anal. Machine Intell., 15(11). (1993) pp:1131-1147

[10] Davatzikos C. and J.L.Prince, An active contour model for mapping the cortex, IEEE Trans. on Medical Imaging, 14(1). (1995) pp :65-80

[11] Davatzikos C. and J.L.Prince (1994) Convexity analysis of active contour models, In Proc. Conf. on Info. Sci. and Sys. pp.:581-587

[12] Abrantes A.J. and J.S.Marques, A class of constrained clustering algorithms for object boundary extraction, IEEE Trans. on Image Processing, 5(11). (1996) pp:1507-1521

[13] Prince J.L. and C.Xu, A new external force model for snakes, In 1996 Image and Multidimensional Signal Processing Workshop. (1996) pp:30-31

[14] Xu C. and J.L.Prince, Gradient Vector Flow Deformable Models, In Handbook of Medical Imaging, Academic Press. (2000) pp: 159-170

[15] Xu C. and J.L. Prince, Snakes, shapes and gradient vector flow, IEEE Trans. on Image Processing, 7(3). (1998) pp:359-369

[16] Tang, Jinshan and S.T. Acton, A DCT based gradient vector flow snake for object boundary detection, Image Analysis and Interpretation, 2004. 6th IEEE Southwest Symposium on. (2004) pp: 157 – 161